

RSC Advances



This is an *Accepted Manuscript*, which has been through the Royal Society of Chemistry peer review process and has been accepted for publication.

Accepted Manuscripts are published online shortly after acceptance, before technical editing, formatting and proof reading. Using this free service, authors can make their results available to the community, in citable form, before we publish the edited article. This *Accepted Manuscript* will be replaced by the edited, formatted and paginated article as soon as this is available.

You can find more information about *Accepted Manuscripts* in the [Information for Authors](#).

Please note that technical editing may introduce minor changes to the text and/or graphics, which may alter content. The journal's standard [Terms & Conditions](#) and the [Ethical guidelines](#) still apply. In no event shall the Royal Society of Chemistry be held responsible for any errors or omissions in this *Accepted Manuscript* or any consequences arising from the use of any information it contains.



Solvate ionic liquid electrolyte with 1,1,2,2-tetrafluoroethyl 2,2,2-trifluoroethyl ether as a support solvent for advanced lithium-sulfur batteries

Received 00th January 20xx,
Accepted 00th January 20xx

DOI: 10.1039/x0xx00000x

Hai Lu,^a Yan Yuan,^b Zhenzhong Hou,^a Yanqing Lai,^c Kai Zhang^c and Yexiang Liu^c

www.rsc.org/

1,1,2,2-tetrafluoroethyl 2,2,2-trifluoroethyl ether (TFTFE) was added to solvate ionic liquid (SIL) based on glyme-lithium salt as a support solvent. The fluorinated ether improves cycle and rate capability of Li-S cells. The key role of TFTFE played in the cell system with SIL is an ionic conduction-enhancing ingredient, especially for high-rate cycle environment.

The issues of energy shortage and environment pollution propel the development of electric vehicles. To cater the strict requests for vehicle-loaded power, all kinds of advanced energy storage devices have been studied extensively.¹ Among these, lithium sulfur (Li-S) battery has attracted worldwide attentions by virtue of its theoretical energy density of up to 2600 Wh kg⁻¹,² which is 10 times higher than that of conventional lithium-ion batteries (LIB). Besides, sulfur has the advantages of non-toxicity and abundance in nature, whereas LIB cathode materials typically contain rare metals.

However, a critical problem originated from redox conversion process of the Li-S batteries is the dissolution of reaction intermediate polysulfides (PS) in the electrolyte.³ The dissolved PS tends to generate repeating shuttle between the cathode and anode,⁴ resulting in low coulombic efficiency and fast self-discharge. Furthermore, the PS can be electrochemically and chemically reduced on Li metal, causing such problems as (a) consuming active species, (b) corroding Li anode, and (c) polarizing Li anode once insoluble products are formed and deposited on the Li surface.⁵ Hence the restrictions towards PS are very necessary for boosting cell performance. Optimizing electrolyte composition is often attempted for this purpose, e.g., altering solvent type, controlling electrolyte amount or introducing functional additives, etc.⁶⁻⁸ However these approaches are still hard to avoid the dissolution and shuttle of PS completely.

Recently, solvate ionic liquid (SIL)⁹ begins to enter the research scope of the Li-S batteries owing to its distinctive structure and properties. The typical case of SIL is the equimolar mixtures of tetraglyme (G4) and certain Li salts (LiX).¹⁰ The formation of complex Li(G4)₂X will weaken the donor ability of G4 solvent because all of the lone pairs of the ether oxygen atoms are donated to the Li⁺ (as we know, the coordination number of Li⁺ is 4~5).¹¹ Thus the PS is poorly solvated in the SIL and quite low solubility of PS can be obtained easily in SIL,¹² which reflects the superiority of SIL applying in the Li-S batteries compared to other electrolyte systems. Research results show that SIL electrolyte allow the cell to have a stable charge-discharge cycles and a coulombic efficiency of greater than 99%.¹² However, the cell capacity is still a bit low over the whole cycling period. Besides, the high viscosity of the SIL gives rise to certain polarization, which is harmful to the potential plateau and rate capability of the cell. Interestingly, It is reported that organo-fluorine compound is capable of enhancing the energy and power density once it was added into the SIL,¹¹ which utilizes the complementary and synergistic actions between SIL and fluorinated ether.

In the study, we aims to select another novel fluorinated ether derivative named 1,1,2,2-tetrafluoroethyl 2,2,2-trifluoroethyl ether (TFTFE) as the support solvent of SIL. Significant improvements of TFTFE-contained electrolyte on electrochemical performances of the Li-S cell are demonstrated here, and the key role of TFTFE in the cell system with SIL is discussed. Several electrolytes using in this experiment were prepared as follows: Lithium bis(trifluoromethane sulfone)imide (LiTFSI, Aldrich) and G4 (Adamas) were mixed at equimolar ratio and magnetically stirred at 50 °C overnight in a argon-filled glove box, forming Li(G4)₂TFSI (LiTFSI:G4=1:1, molar ratio). Then the stoichiometric TFTFE (Adamas) was further added into above Li(G4)₂TFSI to obtain a series of solution mixtures Li(G4)₂TFSI-xTF (LiTFSI:G4:TFTFE=1:1:x, molar ratio, x=1~6).

In general, the required properties of a support solvent for SIL electrolyte Li(G4)₂TFSI in Li-S cells include:¹¹

- Chemical stability against PS;
- Reductive stability against Li metal;
- Miscibility with Li(G4)₂TFSI;
- Better mobility than Li(G4)₂TFSI;

^a School of Materials Science and Engineering, Xi'an University of Science and Technology, Xi'an 710054, China. Email: lhust@126.com

^b School of Metallurgical Engineering, Xi'an University of Architecture and Technology, Xi'an 710055, China

^c School of Metallurgy and Environment, Central South University, Changsha 410083, China

† Electronic Supplementary Information (ESI) available. See DOI: 10.1039/x0xx00000x

- (e) Low donor ability for limiting PS dissolution;
 (f) Weak interaction with solvate structure of $\text{Li}(\text{G4})_1\text{TFSI}$.

We have exhibited for the first time that TTFE is suitable for application in Li-S cells as a co-solvent.¹³ Reversible capacity and coulombic efficiency of the cell can be increased distinctly when TTFE was mixed with conventional ethers. So it is undoubted that TTFE owns favourable chemical stability against PS and reductive stability against Li metal. Meanwhile, the fluorinated ether is miscible with conventional ethers such as G4, thus also can be blended with $\text{Li}(\text{G4})_1\text{TFSI}$. As for the mobility, the conductivity meter (Mettler Toledo, SG3) and viscometer (Brookfield, DV2T-LV) were used for measuring the conductivity and viscosity of the electrolyte, respectively. It is found that $\text{Li}(\text{G4})_1\text{TFSI}$ -4TF has higher ion conductivity and lower viscosity (6.81 ms cm^{-1} and 4.56 mPa s as measured) than $\text{Li}(\text{G4})_1\text{TFSI}$ (1.6 ms cm^{-1} and 81 mPa s as reported¹⁰), which means TTFE favours the improvement of transport property on the basis of SIL.

The fluorinated ether has very low donor ability because it is always too fluorinated to participate in Li^+ solvation.¹⁴ In order to realize the solubility of PS in various electrolytes, S and Li_2S with a molar ratio of 7:1 were mixed and added in each electrolyte (the theoretical content of Li_2S_8 was controlled to be 0.25 mol L^{-1}). As the solubility of PS in the electrolyte has been characterized extensively by observing the colour of the electrolyte containing PS,^{15,16} the pictures of various solutions after different standing time are recorded and compared in Fig.1a. Generally, the normal electrolyte without any PS presents colourless and transparent. However, the colour of $\text{Li}(\text{G4})_1\text{TFSI}$ once adding Li_2S_8 becomes yellow and deepens gradually with time. In principle, the lone pairs of the ether oxygen are all donated to Li^+ in $\text{Li}(\text{G4})_1\text{TFSI}$, and the stable $\text{Li}(\text{G4})_1^+$ complex ion can be formed due to strong ion-dipole interaction between Li^+ and G4.¹⁷ Hence PS dissolves hardly in the SIL. But the above colour change suggests that the solubility of PS still exists to some extent for $\text{Li}(\text{G4})_1\text{TFSI}$. When using TTFE as support solvent, the $\text{Li}(\text{G4})_1\text{TFSI}$ -xTF solution seems lighter than $\text{Li}(\text{G4})_1\text{TFSI}$ at the same standing steps. Especially the colour of $\text{Li}(\text{G4})_1\text{TFSI}$ -4TF is close to colourless and nearly unchanged after standing for 6 days. It suggests that the dissolution of PS is further decreased in the TTFE-contained electrolyte. Moreover, the dissolution quantity of polysulfide decreases gradually as TTFE content in the electrolyte raises (see ESI, Fig.S1 and Fig.S2†). Therefore, more TTFE contributes to weaker dissociation of PS compared to $\text{Li}(\text{G4})_1\text{TFSI}$.

The low donor ability implies that TTFE is hard to overwhelm G4 in Li^+ solvation as well. This speculation can be verified from linear sweep voltammetry (LSV) measurements of stainless steel/Li cells loaded various electrolytes (scanning rate: 0.5 mV S^{-1}). As shown in Fig.1b, the anodic limits of equimolar complex $\text{Li}(\text{G4})_1\text{TFSI}$ is near 5 V vs. Li/Li^+ , exhibiting high oxidative stability of the SILs. After adding TTFE, the LSV curves of $\text{Li}(\text{G4})_1\text{TFSI}$ -xTF move towards low-potential direction slightly. The free ether (G4, in this case), which are not involved in the complex with Li^+ , will be decomposed irreversibly at higher than 4 V vs. Li/Li^+ .¹⁸ The oxidative limits of $\text{Li}(\text{G4})_1\text{TFSI}$ -xTF is very close to that of $\text{Li}(\text{G4})_1\text{TFSI}$, revealing that the majority of complex cations $\text{Li}(\text{G4})_1^+$ still exist steadily and free G4 is scarce in the TTFE-contained system. In other words, the

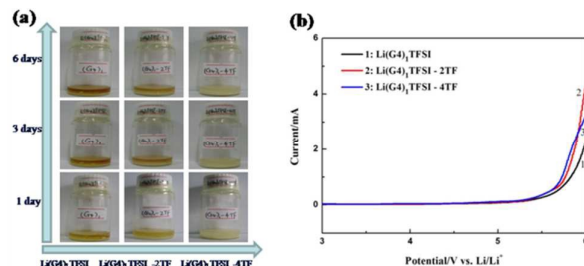


Fig.1 (a) solubility experiments of polysulfides in various electrolytes; (b) LSV measurements of various electrolytes at a scanning rate of 5 mV s^{-1}

distinctive solvate structure of SIL can be reserved although TTFE was introduced into the electrolyte.

It can be seen from the above results that TTFE meets all the demands for support solvent of SIL and can cooperate ideally with it. Next the electrochemical performances of Li-S cells with various electrolytes were investigated. Sulfur-carbon composite (S-C, 79.1% sulfur, see ESI, Fig.S3†) was prepared according to the method described previously¹⁹. Sulfur cathode consisted of 80 wt% S-C composite, 10 wt% carbon black (Super P, Timcal) and 10 wt% poly(vinylidene fluoride) (PVDF, 6020 Solef). The sulfur loading on each cathode was $\sim 1.2 \text{ mg cm}^{-2}$. Coin cells were assembled in the glove box by using above sulfur cathode, Li foil as anode and Advantec GA55 as separator. The electrolyte amount in each cell was controlled to be $\sim 18 \text{ mL g}^{-1}$ (the ratio of electrolyte volume to sulfur content in the cathode).

Firstly, the cyclic voltammetry (CV) for the cell with $\text{Li}(\text{G4})_1\text{TFSI}$ and $\text{Li}(\text{G4})_1\text{TFSI}$ -4TF are presented in Fig.2a and Fig.2b, respectively. The sweep rate is 0.1 mV s^{-1} . All of the cells show two reduction peaks and two very close oxidation peaks (similar to those cases using G4 in electrolyte²⁰). The reduction peaks in cathodic scan stand for the reduction of elemental sulfur to soluble PS and then to the insoluble $\text{Li}_2\text{S}_2/\text{Li}_2\text{S}$, respectively. And the oxidation peaks in anodic scan represent the formation of PS and the final oxidized active sulfur (Li_2S_8 or S), respectively.²⁰⁻²² The CV patterns in the first fourth cycles almost overlap each other, indicating steady cycle ability of the cells with the two electrolytes. It should be noted that the second reduction peak is located at higher value and the voltage gap between oxidation and reduction peaks is smaller for the cell with $\text{Li}(\text{G4})_1\text{TFSI}$ -4TF compared to that for $\text{Li}(\text{G4})_1\text{TFSI}$. TTFE enhances ion conduction of the electrolyte, thus decreases the over-potential and improves reversibility of the cell.

Fig.2c is the initial potential profiles of the Li-S cells with various electrolytes at 0.1 C between 1.5 V and 3 V. Two plateaus can be clearly observed from the discharge curves, corresponding to two-step reaction of sulfur with metallic Li. The low-potential plateau for $\text{Li}(\text{G4})_1\text{TFSI}$ -xTF reaches $\sim 2.1 \text{ V}$, higher than that for $\text{Li}(\text{G4})_1\text{TFSI}$ ($\sim 2.0 \text{ V}$). Meanwhile, the gaps between discharge plateau and charge plateau of the cells containing TTFE is smaller than that using pure SIL. These phenomena are well consistent with above CV results. In addition, initial discharge capacity of the cell increases when the amount of TTFE in the electrolyte increases. Since adding the fluorinated ether can further limit the dissolution of PS at the discharge stage, more active sulfur can be recovered

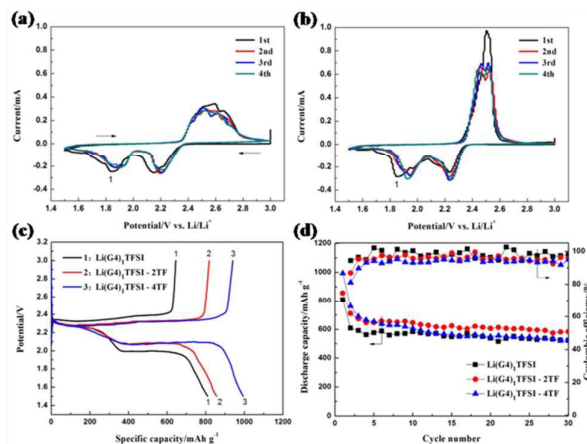


Fig.2 Cyclic voltammogram of the Li-S cell with (a) $\text{Li}(\text{G}4)_1\text{TFSI}$ and (b) $\text{Li}(\text{G}4)_1\text{TFSI-4TF}$ at a sweep rate of 0.1 mV s^{-1} ; (c) initial potential profiles and (d) cycle performances of the cells with various electrolytes at 0.1 C

reversibly during the subsequent charging process.²³ So TTFE is beneficial to the utilization of active material.

The cycle performances of Li-S cells with various electrolytes are shown in Fig.2d (more information seen Fig.S4 in ESI[†]). For the electrolyte containing fluorinated ether, the cell capacity keeps quite stable and the coulombic efficiency approaches 100% after the first cycle, similar to the variation characteristic of the cell with SIL. Obviously, TTFE existing in SIL indeed won't affect inhibition ability of the electrolyte to PS dissolution and shuttle. The relatively low TTFE content contributes to more reversible capacity during the whole cycle period, for instance: a reserved capacity of $\sim 580 \text{ mAh g}^{-1}$ is obtained after 30 cycles for $\text{Li}(\text{G}4)_1\text{TFSI-2TF}$. But it needs to be recognized that the improvement of TTFE to the cell performance is a bit insufficient at the current condition. When continuing to increase TTFE ratio in the SIL, the cycle capability of the cell declines instead, even though the first discharge capacity increases and the coulombic efficiency still keeps in high level. The previous LSV measurement show that the deviation trend enlarges slightly with an increase in TTFE ratio. So adding more TTFE may expand negative effect to SIL structure, which in turn weaken the electrochemical stability of the cell.

The electrochemical performances of the cell at high rate are further investigated. The specific capacities at different discharge rates for various electrolytes are presented in Fig.3a (the charge rate is uniformly 0.1 C). The cell capacities using TTFE-contained electrolytes are always superior to that using pure SIL at each rate. Among them, the cell with $\text{Li}(\text{G}4)_1\text{TFSI-4TF}$ exhibits the best rate capability: stable specific capacities of 480 mAh g^{-1} and 500 mAh g^{-1} can be delivered when the current is elevated to 0.5 C and turned back to 0.3 C after 0.5 C cycles, respectively. Since adding TTFE increases ion conductivity of the electrolyte, the polarization will decline when cell is operated at high-rate conditions. Hence it should be no surprise that the rate performance of the cell is improved remarkably if using TTFE as support solvent.

The cycle capabilities of the cells with various electrolytes at charge/discharge rate of 0.3 C are compared in Fig.3b. The excellent

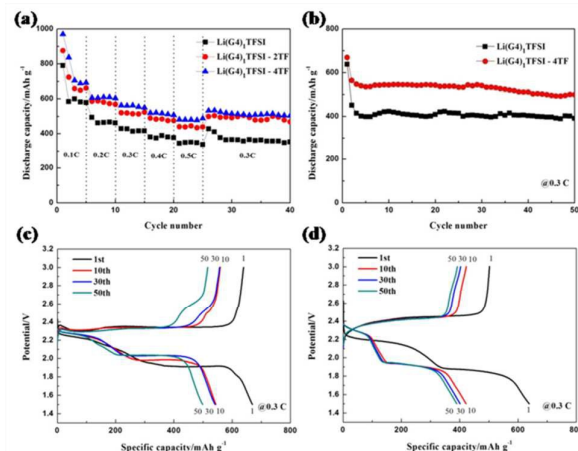


Fig.3 (a) Rate performances of the cells with various electrolytes from 0.1 C to 0.5 C ; (b) cycle performances of the cells with various electrolytes at 0.3 C ; charge-discharge curves of the cell with (c) $\text{Li}(\text{G}4)_1\text{TFSI-4TF}$ and (d) $\text{Li}(\text{G}4)_1\text{TFSI}$ at 0.3 C

cycle stability appears in the cell with $\text{Li}(\text{G}4)_1\text{TFSI-4TF}$. The capacity retention after 50 cycles is up to 88.3% based on the second discharge. Moreover, $\text{Li}(\text{G}4)_1\text{TFSI-4TF}$ allow the cell to release more capacities than $\text{Li}(\text{G}4)_1\text{TFSI}$ during cycling. The difference of cell performance between two kinds of electrolytes at high rate is more noticeable than that at low rate. Besides, the discharge plateau for $\text{Li}(\text{G}4)_1\text{TFSI-4TF}$ also overtops $\text{Li}(\text{G}4)_1\text{TFSI}$ at initial cycle (see ESI, Fig.S5[†]), demonstrating less over-potentials in the former. The plateau potential ascends step by step and then maintains stable during subsequent cycles in the case of $\text{Li}(\text{G}4)_1\text{TFSI-4TF}$ (Fig.3c), which reveals the achievement of a stable electrochemical environment needs a procedure, like other electrolytes using abundant fluorinated ether.²⁰ While the discharge plateau for $\text{Li}(\text{G}4)_1\text{TFSI}$ is stable all the time (Fig.3d). Therefore, the polarization gap between two electrolytes is further enlarged at latter cycles.

To better understand the function of TTFE in the cell system, the electrochemical impedance spectroscopy (EIS) of the Li-S cells with various electrolytes was examined. The frequency range of the measurement was $10^5 \sim 0.1 \text{ Hz}$, with the perturbation amplitude of 5 mV . The impedance plots before cycle are composed of a semicircle in medium-to-high frequency and an inclined line in the low frequency (Fig.4a). The former is attributed to the interface charge-transfer resistance (R_{ct}), and the latter corresponds to Warburg impedance (W_o , associated with Li^+ diffusion in the active material). The high-frequency intercept on the real axis represents the ohmic resistance (R_o), including the electrolyte and electrode resistances.²⁴ After 50 cycles, the impedance responses are divided into two obvious semicircles (Fig.4b). The additional semicircle in the high frequency is related to solid-electrolyte interface (SEI) film formed during the charge-discharge process (R_{se}).^{25,26} The fitted resistance data according to the corresponding equivalent circuit are shown in Table 1.

The R_o for the cell with fluorinated ether is obviously smaller than the one without it, which is another convincing evidence of TTFE on promoting ion transport of the electrolyte. The decline in R_{ct} for $\text{Li}(\text{G}4)_1\text{TFSI-4TF}$ compared to $\text{Li}(\text{G}4)_1\text{TFSI}$ suggests that the

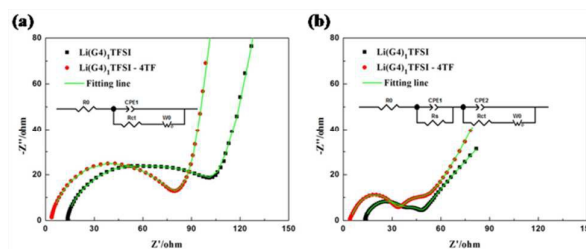


Fig.4 EIS plots of Li-S cells with various electrolytes (a) before cycle and (b) after cycles

Table 1 Fitted resistances data from the equivalent circuit

Electrolyte	Stage	R_0 (Ω)	R_s (Ω)	R_{ct} (Ω)
Li(G4) ₁ TFSI	before cycle	11.36	/	80.64
	after cycles	12.84	25.23	8.78
Li(G4) ₁ TFSI-4TF	before cycle	2.57	/	70.71
	after cycles	4.25	30.66	6.41

electrolyte containing TTFE is capable of wetting the electrode sufficiently and improving the electrochemical reaction within the cell.^{14,25} The increase in R_s is probably associated with film building of TTFE on Li anode, which can block the access of PS to metallic Li and side-reactions between them.¹³ However, whether modified surface film or further reduced PS dissolution should be minor contributing factor for improving cell performance in the high concentration electrolytes, considering that the dissolution and shuttle of PS have already been negligible at this moment. Combining the resistance data with previous electrochemical tests, it can be concluded that the more important role of TTFE played in the cell system using SIL should be an ionic conduction-enhancing ingredient, especially for high-rate cycle environment.

In summary, we have investigated the effects of adding fluorinated ether on the basic properties of SIL electrolyte and electrochemical performance of Li-S cells. TTFE meets the demands for support solvent of SIL, including favourable mobility, low dissolution ability of PS and weak interaction with solvate structure, thus is suitable for cooperating with SIL. The cell using the fluorinated ether owns higher reversible capacity than the one without it, accompanied by coulombic efficiency near 100% and quite stable cycle capability. Especially, the low polarization and excellent performance are exhibited in the high-rate measurement of the cell with TTFE. The capacity retention after 50 cycles is up to 88.3% based on the second discharge at 0.3 C charge-discharge test for Li(G4)₁TFSI-4TF. Here, the enhanced ion conduction by TTFE is mainly contributive for the improvement of the cell performance.

Acknowledgements

The authors thank the financial support of the National Natural Science Foundation of China (No.21204072). We also thank the support of viscosity measurement provided by the Analytical & Testing Center, Material & Industrial Technology Research Institute, Beijing.

Notes and references

- L. Li, Z. Wu, S. Yuan and X.-B. Zhang, *Energy Environ. Sci.*, 2014, 7, 2101-2122.
- M. K. Song, E. J. Cairns and Y. Zhang, *Nanoscale*, 2013, 5, 2186-2204.
- M. Barghamadi, A. S. Best, A. I. Bhatt, A. F. Hollenkamp, M. Musameh, R. J. Rees and T. R  ther, *Energy Environ. Sci.*, 2014, 7, 3902-3920.
- Y. V. Mikhaylik and J. R. Akridge, *J. Electrochem. Soc.*, 2004, 151, A1969-A1976.
- S. S. Zhang, *J. Power Sources*, 2013, 231, 153-162.
- S. Yoon, Y.-H. Lee, K.-H. Shin, S. B. Cho and W. J. Chung, *Electrochim. Acta*, 2014, 145, 170-176.
- X.-B. Cheng, J.-Q. Huang, H.-J. Peng, J.-Q. Nie, X.-Y. Liu, Q. Zhang and F. Wei, *J. Power Sources*, 2014, 253, 263-268.
- F. Wu, J. Qian, R. Chen, J. Lu, L. Li, H. Wu, J. Chen, T. Zhao, Y. Ye and K. Amine, *ACS Appl. Mater. Interfaces*, 2014, 6, 15542-15549.
- T. Mandai, K. Yoshida, K. Ueno, K. Dokko and M. Watanabe, *Phys. Chem. Chem. Phys.*, 2014, 16, 8761-8772.
- K. Ueno, K. Yoshida, M. Tsuchiya, N. Tachikawa, K. Dokko and M. Watanabe, *J. Phys. Chem. B*, 2012, 116, 11323-11331.
- K. Dokko, N. Tachikawa, K. Yamauchi, M. Tsuchiya, A. Yamazaki, E. Takashima, J. W. Park, K. Ueno, S. Seki, N. Serizawa and M. Watanabe, *J. Electrochem. Soc.*, 2013, 160, A1304-A1310.
- C. Zhang, A. Yamazaki, J. Murai, J.-W. Park, T. Mandai, K. Ueno, K. Dokko and M. Watanabe, *J. Phys. Chem. C*, 2014, 118, 17362-17373.
- H. Lu, Y. Yuan, K. Zhang, F. Qin, Y. Lai and Y. Liu, *J. Electrochem. Soc.*, 2015, 162, A1460-A1465.
- M. Cuisinier, P. E. Cabelguen, B. D. Adams, A. Garsuch, M. Balasubramanian and L. F. Nazar, *Energy Environ. Sci.*, 2014, 7, 2697-2705.
- L. Suo, Y. Hu, H. Li, M. Armand and L. Chen, *Nat. Commun.*, 2013, 4, 1481.
- N. Azimi, Z. Xue, I. Bloom, M. L. Gordin, D. Wang, T. Daniel, C. Takoudis and Z. Zhang, *ACS Appl. Mater. Interfaces*, 2015, 7, 9169-9177.
- C. Zhang, K. Ueno, A. Yamazaki, K. Yoshida, H. Moon, T. Mandai, Y. Umebayashi, K. Dokko and M. Watanabe, *J. Phys. Chem. B*, 2014, 118, 5144-5153.
- K. Yoshida, M. Nakamura, Y. Kazue, N. Tachikawa, S. Tsuzuki, S. Seki, K. Dokko and M. Watanabe, *J. Am. Chem. Soc.*, 2011, 133, 13121-13129.
- J. Li, F. Qin, L. Zhang, K. Zhang, Q. Li, Y. Lai, Z. Zhang and J. Fang, *J. Mater. Chem. A*, 2014, 2, 13916-13922.
- H. Lu, K. Zhang, Y. Yuan, F. Qin, Z. Zhang, Y. Lai and Y. Liu, *Electrochim. Acta*, 2015, 161, 55-62.
- Y.-S. Su and A. Manthiram, *Electrochim. Acta*, 2012, 77, 272-278.
- Z. Dong, J. Zhang, X. Zhao, J. Tu, Q. Su and G. Du, *RSC Adv.*, 2013, 3, 24914-24917.
- Y. Diao, K. Xie, X. Hong and S. Xiong, *Acta Chim. Sinica*, 2013, 71, 508-518.
- F. Qin, K. Zhang, J. Fang, Y. Lai, Q. Li, Z. Zhang and J. Li, *New J. Chem.*, 2014, 38, 4549-4554.
- Q. Li, Z. Zhang, K. Zhang, J. Fang, Y. Lai and J. Li, *J. Power Sources*, 2014, 256, 137-144.
- X. Cui, Z. Shan, L. Cui and J. Tian, *Electrochim. Acta*, 2013, 105, 23-30.